energies

MDPI

Article

Influence of Clay Content on CO_2-Rock Interaction and Mineral-Trapping Capacity of Sandstone Reservoirs

Emad A. Al-Khdheeawi [1,2,*], Doaa Saleh Mahdi [2], Yujie Yuan [1,3,4] and Stefan Iglauer [4]

[1] Western Australian School of Mines: Minerals, Energy and Chemical Engineering, Curtin University, Perth, WA 6845, Australia
[2] Oil and Gas Engineering Department, University of Technology-Iraq, Baghdad 10066, Iraq
[3] School of Earth Sciences, Yunnan University, Kunming 650500, China
[4] School of Engineering, Edith Cowan University, Joondalup, WA 6027, Australia
* Correspondence: 150070@uotechnology.edu.iq or e.al-khdheeawi@graduate.curtin.edu.au

Abstract: The injection of carbon dioxide (CO_2) is an essential technology for maximizing the potential of hydrocarbon reservoirs while reducing the impact of greenhouse gases. However, because of the complexity of this injection, there will be many different chemical reactions between the formation fluids and the rock minerals. This is related to the clay content of sandstone reservoirs, which are key storage targets. Clay content and clay types in sandstone can vary substantially, and the influence of these factors on reservoir-scale CO_2-water-sandstone interactions has not been managed appropriately. Consequently, by simulating the process of CO_2 injection in two different clay-content sandstones (i.e., high- and low-clay content), we investigated the effect of the sandstone clay concentration on CO_2-water-sandstone interactions in this article. High clay content (Bandera Grey sandstone) and low clay content (Bandera Brown sandstone) were considered as potential storage reservoirs and their responses to CO_2 injection were computationally assessed. Our results indicate that the mineralogical composition of the sandstone reservoir significantly varies as a result of CO_2-water-sandstone interactions. Clearly, the high clay-content sandstone (Bandera Grey) had a higher maximum CO_2 mineral-trapping capacity (6 kg CO_2/m^3 sandstone) than Bandera Brown Sandstone (low clay content), which had only 3.3 kg CO_2/m^3 sandstone mineral-storage capacity after 400 years of storage. Interestingly, pH was decreased by ~3 in Bandera Grey sandstone and by ~2.5 in Bandera Brown sandstone. Furthermore, porosity increased in Bandera Grey sandstone (by +5.6%), more than in Bandera Brown Sandstone (+4.4%) after a 400-year storage period. Overall, we concluded that high clay-content sandstone shows more potential for CO_2 mineral-trapping.

Keywords: rock interactions; clay content; porosity evolution; mineral-trapping; mineral precipitation; mineral dissolution; CO_2 storage; reservoir simulation

Citation: Al-Khdheeawi, E.A.; Mahdi, D.S.; Yuan, Y.; Iglauer, S. Influence of Clay Content on CO_2-Rock Interaction and Mineral-Trapping Capacity of Sandstone Reservoirs. *Energies* **2023**, *16*, 3489. https://doi.org/10.3390/en16083489

Academic Editors: Federica Raganati and Paola Ammendola

Received: 24 February 2023
Revised: 14 April 2023
Accepted: 15 April 2023
Published: 17 April 2023

1. Introduction

The concentration of greenhouse gases today is mostly caused by anthropogenic activities, with atmospheric CO_2 emissions making up around 63% of this concentration. The burning of natural fuels and industrial processes, as well as land clearing, are the main sources that contribute to the global increase in CO_2 concentrations [1]. The CO_2 capture and storage (CCS) technique is the most promising technical way to reduce atmospheric CO_2 emissions. CCS consists of two stages: pre-combustion CO_2 collecting and geological CO_2 storage in underground geological reservoirs. CO_2 injection is an important strategy for improving oil recovery and lowering the emissions of greenhouse gases into the environment, which involves trapping CO_2 from large stationary sources such as the burning of fossil fuels, solid fuels, and heat sources as well as power-generation processes. This CO_2 is then injected into deep storage sites such as deep coal beds, oil and gas reservoirs, and aquifers, in its supercritical phase [2,3]. Due to a number of factors, including the

well-understood geology during oil and gas exploration operations, the widespread use of CO_2 injection into oil and gas reservoirs to enhance hydrocarbon recovery, and the availability of the surface and underground infrastructure, which can be used to inject CO_2 for geo-sequestration purposes, depleted oil and gas reservoirs are considered to be very economical carbon geo-sequestration sites [4]. Injecting CO_2 into oil and gas reservoirs hence increases the production of hydrocarbons while lowering CO_2 emissions. According to estimates, depleted oil reservoirs have the ability to store about 60% of the CO_2 that is pumped into them. However, about 40% of the CO_2 that is injected is produced using oil, which can then be reinjected into an oil reservoir [5]. Another key solution to lower CO_2 emissions to the atmosphere is CO_2 sequestration in unmineable coal seams [6]. Lately, enhanced coal-bed methane (ECBM) recovery and CO_2 sequestration in unmineable coal seams have garnered a great deal of attention [7]. The capacity of this technology to produce methane in addition to long-term CO_2 sequestration, especially in coals with high methane contents, helps to lower the cost of the CO_2 sequestration process [8]. Due to its higher affinity to adsorb into coal than methane, the injected CO_2 into deep unmineable coal formations physically adsorbs in the coal surface and displaces the existing methane. At depths of more than 800 m, deep saline aquifers, porous layers of rock, often contain formation waters of a high salinity that are of no use to industry. Deep saline aquifers are the most desired CO_2 storage sinks, as they have the highest CO_2 storage capacity when compared to other CO_2 geological sinks. For efficiency and safety reasons, CO_2 must be injected into deep saline aquifers at depths of more than 800 m. At these depths, the associated temperature (31.04) and pressure (7.39 MPa) conditions keep the CO_2 in a supercritical phase, where it can remain for an extended period of time [9]. Due to their great CO_2 storage capability, deep saline aquifers are regarded as the best storage formations [10]. The injected CO_2 tends to move vertically because of its low density compared to formation brine. Different CO_2 trapping mechanisms, such as physical trapping, hydrodynamic trapping, and chemical trapping might limit this undesirable vertical CO_2 migration [3]. The injected CO_2 is trapped in physical trapping as residual trapping [11,12] and structural trapping [13]. In residual trapping, sometimes referred to as capillary trapping, which may quickly store enormous volumes of CO_2, a specific (non-wetting) phase is moved away from the center of the rock pore by an immiscible (wetting) phase, resulting in the formation of a residual phase. After that, capillary forces will cause a sizable portion of the CO_2 to be trapped in the tiny pore spaces. The capacity of residual trapping is influenced by a number of variables, including interfacial tension, wettability, initial gas saturation, residual saturation, pore geometry and hysteresis [11,12]. In structural trapping, the CO_2 is trapped below impermeable (or extremely low permeability) caprock by a primary and physical trapping mechanism. Commonly, CO_2 is trapped below the caprock because the capillary forces exerted by these extremely low-permeability seals are greater than the buoyancy forces. In any geological storage deposit, structural trapping is crucial because it stops CO_2 leakage while waiting for additional storage mechanisms to begin working [13]. When CO_2 migrates slowly over long distances, some of it will be trapped by a hydrodynamic trapping mechanism [3]. This CO_2 dissolution in water creates a CO_2-enriched solution with a high density that permanently settles in the formation. The CO_2–water interface area affects the diffusion in the dissolution trapping, thus increasing the CO_2–water area of contact will increase the quantity of CO_2 dissolved in water. Moreover, a number of variables, such as the reservoir's temperature, pressure, and salinity, have an impact on solubility trapping. Dissolution-trapping is a laborious process that takes between 100 and 1000 years to complete [14].

According to the chemical mechanism, a portion of the injected supercritical CO_2 will dissolve in brine, creating carbonic acid [15,16]. It could subsequently interact with the minerals in the reservoir rocks and become trapped as a secondary mineral [17–19]. Because mineral-trapping can hold the CO_2 for a very long time, it is regarded as an appealing trapping technique.

When carbon dioxide (CO_2) is injected into depleted oil reservoirs, the formation rock and newly generated in situ solutes (carbonated brine) frequently interact chemically [18,20,21]. The reservoir's permeability, porosity, and capillary pressure may be impacted by the mineral dissolution–precipitation caused by the interactions between rock, water, and CO_2 [20–22] and therefore have an impact on the CO_2 storage and the movement of CO_2 via porous media [22,23]. Importantly, sandstone reservoirs are estimated to be significant CO_2 storage locations. Because of their higher quartz content than carbonate rocks, sandstone rocks were generally perceived to be less reactive with CO_2 [24,25]. However, in addition to quartz, sandstones frequently include a substantial amount of cementing and clay elements [26,27]. When these elements come into contact with CO_2, they will interact and dissolve. For example, Xie et al. [28] found that injecting CO_2 moderately increased the permeability of the sandstone while slightly affecting its porosity. In addition, CO_2 injection leads to the reduction of the rock's permeability by 15 to 30% because of either mineral participation or fine migration [29]. Furthermore, laboratory measurements on sandstone samples indicate that the sample permeability is reduced because dissolving of the cementing material in the sandstone causes the movement of dislodged quartz and clay and the sealing of pore spaces close to the sample discharge [30]. Additionally, it was found that this sandstone is subjected to mineral migration and dissolution at various permeabilities [31]. Porosity and permeability variation due to CO_2 injection is a function of reservoir rock mineral composition. In comparison to their carbonate counterparts, reactive minerals were predicted to be less abundant in sandstone deposits. However, because various sandstone rocks contain varied amounts of clay, the evolution of rock properties may vary.

Although clay contents are varied substantially in various sandstones, the impact of the clay content on the reservoir scale CO_2-water-rock interactions, brine pH, porosity evolution and mineral-trapping capacity have not been well understood.

Thus, in this paper, a three-dimensional model was used to study the impact of clay content on porosity variation and mineral-trapping capacity during CO_2 sequestration using two different sandstones (i.e., high clay-content sandstone represented by Bandera Grey Sandstone and low clay-content sandstone represented by Bandera Brown Sandstone).

2. Materials and Methods

In order to examine the influence of clay content on the interactions between CO_2, water, and rocks during CO_2 injection, a three-dimensional reservoir simulation model was constructed using two different clay-content reservoirs (i.e., high clay (Bandera Grey) and low clay content (Bandera Brown) sandstone reservoirs). The numerical simulation software TOUGHREACT-ECO2N for multicomponent, chemically reactive, non-isothermal, and multiphase flow was employed [32]. TOUGHREACT can be used in 1–3 D geologic models having chemical and physical heterogeneity and can be used in a variety of subsurface settings. The range of the EOS module in use and the range of the chemical thermodynamic database that is applicable govern the temperature (T) and pressure (P) ranges. The thermodynamic database is the only restriction on the temperature and pressure range. From absolutely dry to thoroughly saturated, water saturation can vary. The model can handle water with diluted to moderately salty ionic strengths (up to 6 molal for an NaCl-dominant solution). All pH and Eh conditions can be handled with TOUGHREACT. H_2O-NaCl-CO_2 mixtures' thermodynamic and thermophysical properties are calculated using the ECO2N equation of state [33,34] using Spycher and Pruess correlations [15], which can be applied for a very wide range of reservoir conditions (i.e., reservoir temperature of 283.15 K $\leq$ T $\leq$ 383.15 K; reservoir pressure of P $\leq$ 60 MPa; and salinity of zero $\leq$ salinity $\leq$ fully saturated. ECO2N can be used to model the isothermal and non-isothermal flow processes of liquids, gases, and two-phase mixtures. In TOUGHREACT, the main mechanisms for the movement of fluids and heat include the following: fluid flow in both the liquid and gas phases is governed by pressure, viscous, and gravity forces; interactions between flowing phases are depicted by characteristic curves (relative permeability

and capillary pressure); heat transfer is by conduction and convection; and diffusion of water vapor and non-condensable gases is included. Temperature-dependent thermophysical and geochemical parameters, such as fluid (gas and liquid) density and viscosity, as well as thermodynamic and kinetic information for mineral-water-gas processes, are estimated.

The model's dimensions were 1000 m long, 1000 m wide, and 1000 m thick (depth from 1000 m to 2000 m; Figure 1). The model consisted of 11,250 uniformly spaced grids. The initial reservoir pressure was set to be 15 MPa at the center of the model (at depth of 1500 m). The model was assumed to be isothermal with a temperature of 60 °C. To simulate a constant boundary pressure conditions on lateral and bottom faces of the model, the volume of the outer boundary cell was doubled by a multiplier of 10^8 [35]. Initially, the aquifer was completely saturated with brine, which had a salinity of 30,000 ppm NaCl. The aquifer brine was pre-equilibrated with the minerals existing in the aquifer before the CO_2 injection. Thus, the initial aquifer brine pH was 7.43 and the chemical composition of the brine was Ca^{2+}, Cl^-, Fe^{2+}, H^+, H_2O, Hco^{3-}, K^+, Mg^{2+}, Na^+, $Sio_2(Aq)$, So_4^{2-}, and Alo^{2-}. Quantitative X-ray diffraction was used to measure the three various mineralogical compositions used to simulate the Bandera Grey sandstone, Bandera Brown sandstone, and the shale layer (Table 1).

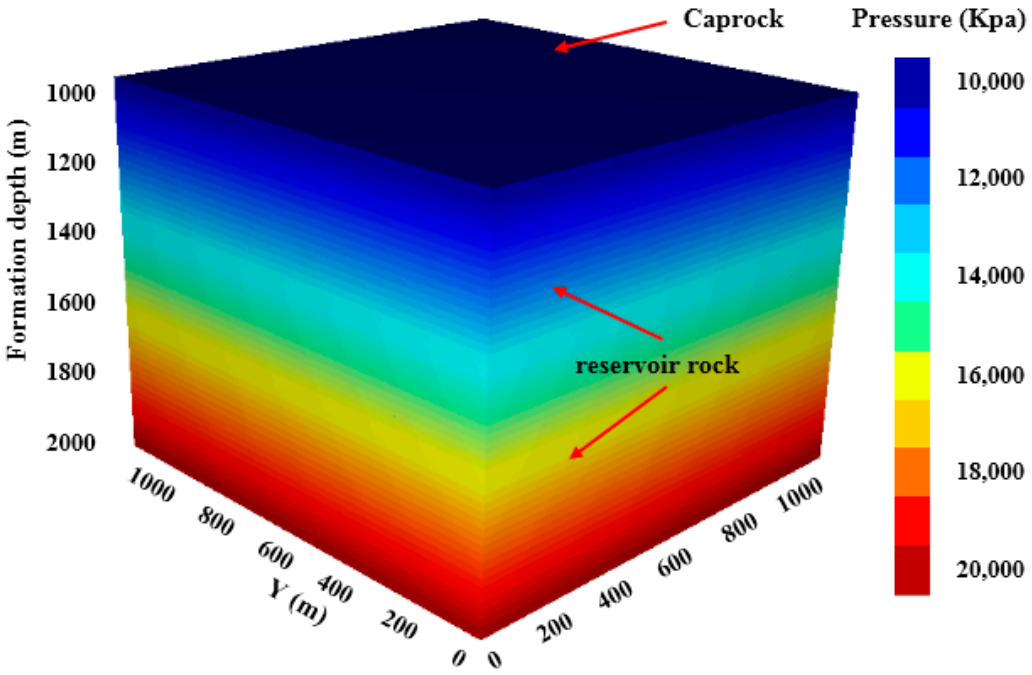

Figure 1. The developed simulation model showing the reservoir pressure distribution.

For both Bandera Grey and Bandera Brown sandstone scenarios, with a constant injection rate of 1000 Kton per year for ten years, 10,000 Kton of CO_2 was injected near the bottom depth of the reservoir model.

We then calculated the capacity of mineral-trapping, rock interactions, and the corresponding changes in reservoir porosity and pH over a 400-year post-injection period.

Previous research clearly demonstrated that the used relative permeability and capillary pressure curves affect the results of CO_2 injection simulations [36,37]. Importantly, these curves also depend on the wettability of the rock [37–39]. In order to model the wettability of sandstone, we used relative permeability and capillary pressure curves (Figure 2) of a water-wet rock that were developed previously by [37,38]. The hysteresis in these curves was represented by importing the endpoints parameters listed in Table 2 into the van Genuchten–Mualem model [40,41]:

$$S^* = (\mathrm{S_w} - S_{wr})/(S_{ws} - S_{wr}), \hat{\mathrm{S}} = (\mathrm{S_w} - S_{wr})/(1 - S_{wr} - S_{gr}) \quad (1)$$

$$(P_{cap}) = P_0\left([S^*]^{-1/\lambda} - 1\right)^{1-\lambda} \quad (2)$$

$$k_{rg} = \left(1 - \hat{\mathrm{S}}\right)^2\left(1 - \hat{\mathrm{S}}^2\right) \text{ when } S_{gr} > 0 \quad (3)$$

$$k_{rg} = 1 - k_{rw} \text{ when } S_{gr} = 0 \quad (4)$$

$$k_{rw} = 1 \text{ when } S_w \geq S_{ws} \quad (5)$$

$$k_{rw} = \sqrt{S^*}\left\{1 - \left(1 - [S^*]^{1/\lambda}\right)^{\lambda}\right\}^2 \text{ when } S_w < S_{ws} \quad (6)$$

where: k_{rg} is the CO_2 relative permeability, k_{rw} is the water relative permeability, S_{gr} is the CO_2 residual saturation, S_w is the water saturation, S_{ws} is the saturated water saturation (=1), S_{wr} is the water residual saturation, P_c is the capillary pressure, P_0 = capillary pressure scaling factor, λ is the pore-size distribution index (fitting parameter).

Table 1. The used mineral composition and kinetics parameters for the various rock types.

Minerals Volume Fraction %				Kinetic Parameters		
Mineral	**Bandera Grey Sandstone**	**Bandera Brown Sandstone**	**Shale**	**Kinetic Constant**	**Activation Energy**	**Specific Surface Area**
quartz	58.0	74.4	60.0	1.023×10^{-14}	87.7	9.8
Kaolinite	7.00	2.60	0.00	6.918×10^{-14}	22.2	151.6
Chlorite	6.00	2.30	6.00	3.02×10^{-13}	88	151.6
illite	0.00	0.00	7.00	1.660×10^{-13}	35	151.6
ankerite	15.0	0.00	12.0	1.260×10^{-9}	62.76	9.8
calcite	0.00	5.10	9.00	Equilibrium		
albite	12.2	9.00	6.00	2.754×10^{-13}	69.8	9.8
dolomite	0.00	1.20	0.00	2.951×10^{-8}	52.2	9.8
k-feldspar	0.00	1.50	0.00	3.890×10^{-13}	38	9.8
muscovite	1.80	3.90	0.00	1.0×10^{-14}	58.48	151.6

Table 2. Van Genuchten–Mualem model parameters used for simulating sandstone Pc and Kr curves.

Process	**Relative Permeability**			**Capillary Pressure**			
	Sgr	**Swr**	**λ**	**Swr**	**λ**	**P_0 [Pa]**	**Pmax [Pa]**
CO_2 injection	0	0.25	1.05	0.249	0.7	1500	20,000
Post-injection	0.30	0.25	0.95	0.249	0.51	1000	20,000

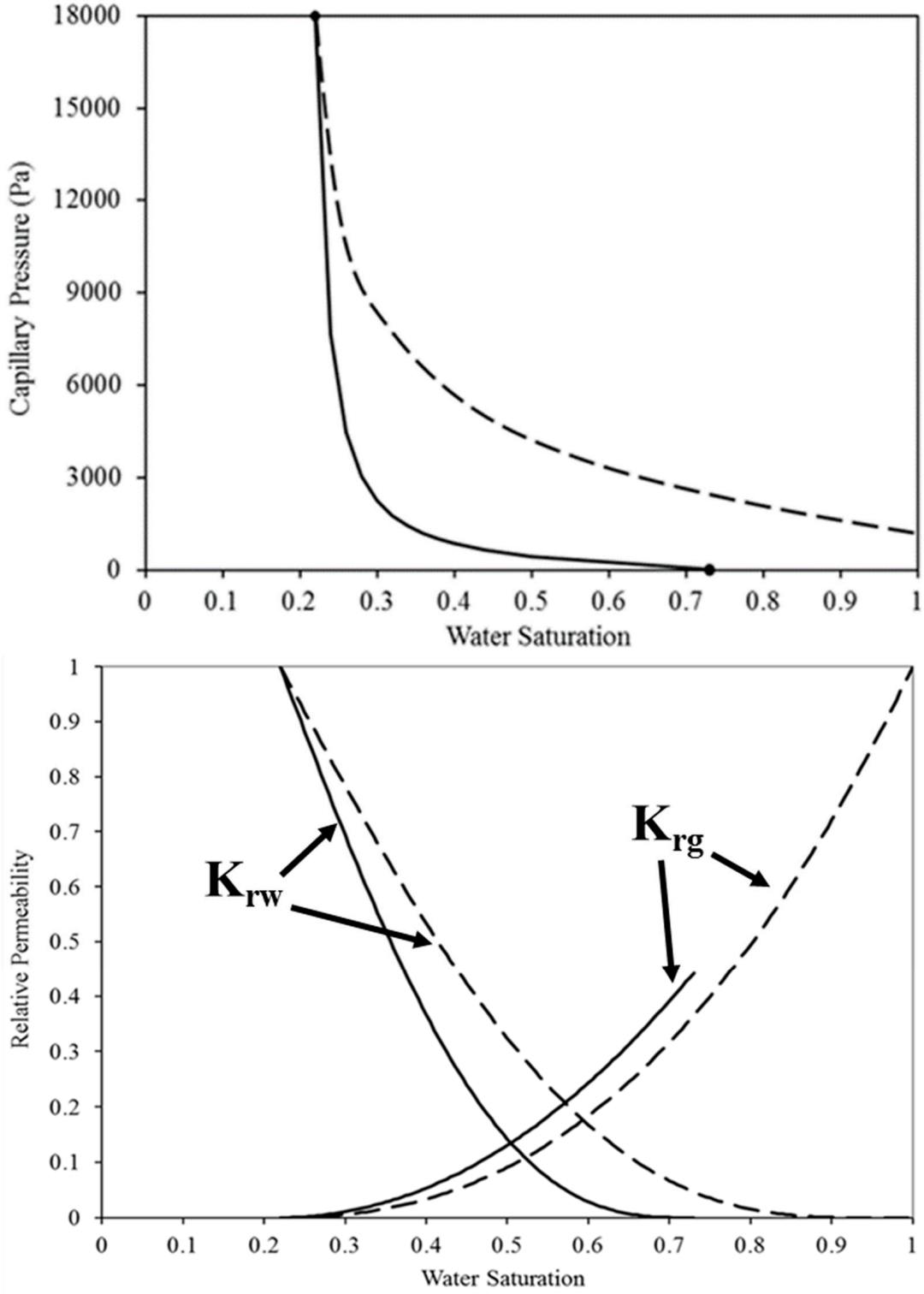

Figure 2. The imported Pc (**top**) and relative permeability (**bottom**) curves for the sandstone rocks. Dashed lines represent the CO_2 injection process and solid lines represent the post-injection process.

3. Results and Discussion

3.1. Effect of Clay Content on CO_2-Mineral Interaction

The complicated nature of underground CO_2 injection will create a variety of chemical reactions between the formation fluids and the rock minerals. Since sandstone reservoirs are important storage goals, this is connected to their clay content. The influence of these

elements on the reservoir scale CO_2-water-sandstone interactions has not been properly handled, and clay content and clay type in sandstone can vary significantly. In this section, we examined the impact of sandstone clay concentration on CO_2-water-sandstone interactions by simulating the process of CO_2 injection in two distinct sandstones with varied clay contents (high and low clay content).

Figures 3–6 show the progression of changes in the volume fraction of minerals (dissolution-precipitation), the CO_2 Sequestered in minerals, change in pH, and the associated changes in porosity, as a function of storage time (0–400 years) for high clay-content (Bandera Grey) and low clay-content (Bandera Brown) sandstone reservoirs. Our findings showed that clay content has a significant effect on these CO_2-water-sandstone interactions; for both sandstone types, kaolinite, illite, quartz and ankerite are precipitated, and chlorite, muscovite, and albite are dissolved, in different quantities. Additionally, the results showed that k-feldspar and dolomite are dissolved, and calcite is precipitated in Bandera Brown Sandstone (Figure 3). Importantly, the results indicated that kaolinite, Illite, and ankerite have higher precipitation rates in the Bandera Grey sandstone compared to their precipitation rates in the Bandera Brown, while the precipitation of quartz is higher in the Bandera Brown sandstone. However, muscovite and Albite have higher dissolution rates in the Bandera Brown sandstone compared to their dissolution rates in the Bandera Grey, while the dissolution of chlorite is higher in the Bandera Grey sandstone. Also, the results demonstrated that chlorite has the greatest variation in mineral volume fraction in Bandera Grey sandstone (22.4% of the initial chlorite volume is dissolved), while albite has the highest variation in volume fraction of mineral in Bandera Brown sandstone (23.9% of the initial albite volume is dissolved; Figure 3). Significantly, these results are in line with the chemical equations of the reactions of sandstone minerals. For instance, the below equations show the reactions of muscovite, albite, and chlorite with the carbonic acid will let to dissolving these minerals and forming Kaolinite:

$$\underset{\text{Muscovite}}{2K\,AlSi_3O_8} + 2H_2CO_3 + 9H_2O \leftrightarrows 2K^+ + 2HCO_3^- + \underset{\text{Kaolinite (clay)}}{Al_2Si_2O_5(OH_4)} + \underset{\text{Silica acid}}{4H_4SiO_4} \quad (7)$$

$$\underset{\text{Albite}}{2Na\,AlSi_3O_8} + 2H_2CO_3 + 9H_2O \leftrightarrows 2Na^+ + 2HCO_3^- + \underset{\text{Kaolinite (clay)}}{Al_2Si_2O_5(OH_4)} + \underset{\text{Silica acid}}{4H_4SiO_4} \quad (8)$$

$$\underset{\text{Chlorite}}{Fe_{2.5}Mg_{2.5}Al_2Si_3O_{10}(OH)_8} + \underset{\text{Calcite}}{2.5CaCO_3} + 5CO_2 \leftrightarrows \underset{\text{Siderite}}{2.5FeCO_3} + 2H_2O + \underset{\text{Kaolinite}}{Al_2Si_2O_5(OH_4)} + \underset{\text{Dolomite}}{2.5MgCa(CO_3)_2} + SiO_2 \quad (9)$$

3.2. Effect of Clay Content on PH Variation

It is clearly shown in the study that PH has an important influence on CO_2 dissolution in formation water and that PH reduction leads to increasing CO_2 dissolution. Thus, in this section we studied the effect of the clay content of sandstone reservoirs on PH variation during CO_2 sequestration. Figure 4 presents the PH variation during long-term (400 years) storage for two different clay-content sandstones. Our results also showed that clay content affects the pH reduction in the sandstone reservoir during the CO_2 storage process. The pH was dropped by ~3 units for the Bandera Grey sandstone and by ~2.5 for the Bandera Brown sandstone scenario at the end of the storage period (400 years; Figure 4).

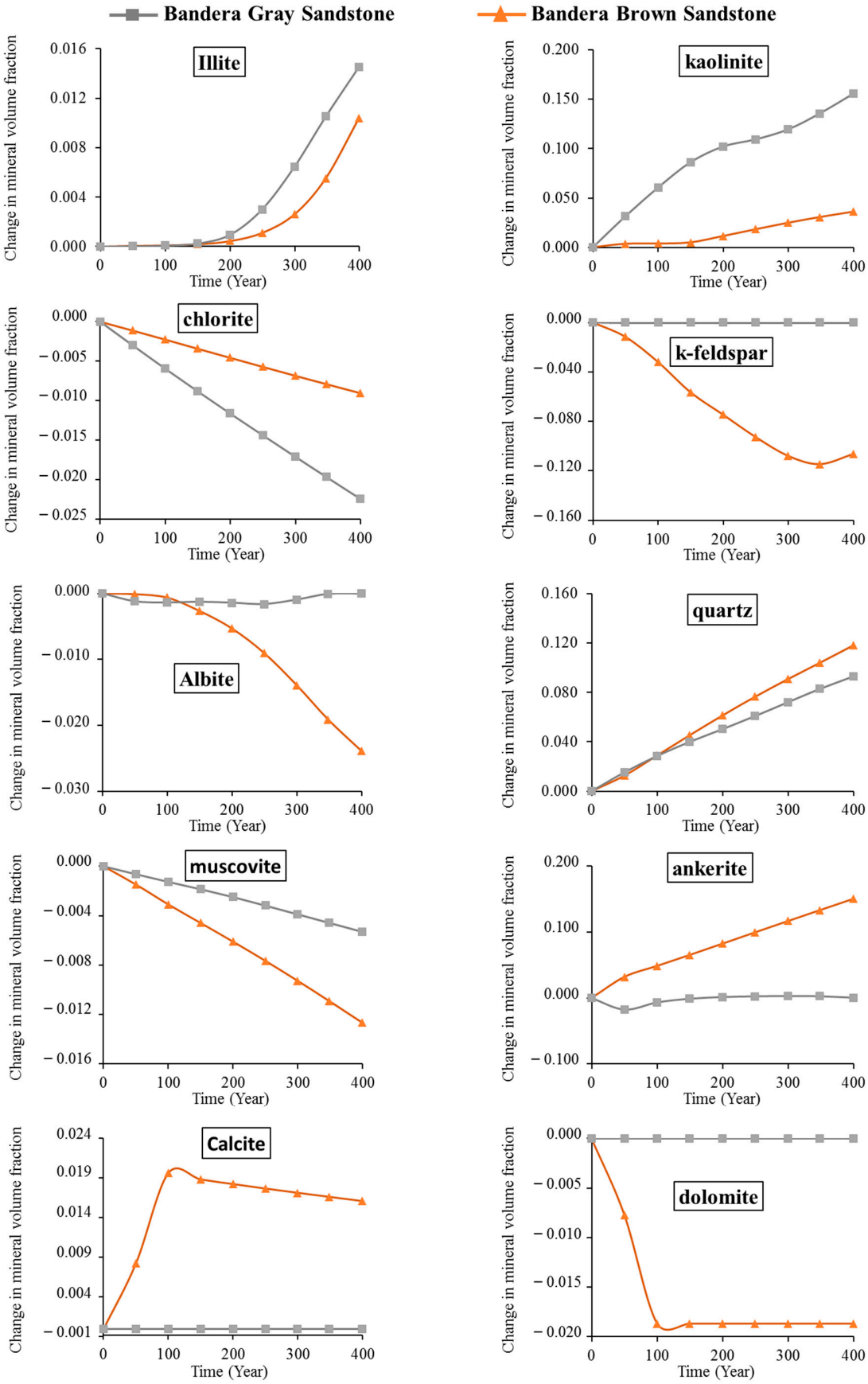

Figure 3. Changes in mineral abundance for different clay-content sandstones with storage time.

3.3. Effect of Clay Content on Mineral CO_2 Storage

In the geologic formation, CO_2 can interact directly or indirectly with minerals and organic matter, causing organic materials dissolution and carbonates precipitation. Then, this dissolution process can lead to a long-term CO_2 trapping mechanism (i.e., mineral-trapping). due to its ability to hold CO_2 for a very long time, mineral-trapping regarded as a desirable trapping mechanism. Figure 5 shows the CO_2 stored as mineral for the high and low clay-content sandstones after 400 years post-injection time. Our results indicated that the clay content of sandstone highly affects the mineral CO_2 storage. The results show that Bandera Grey Sandstone has a higher mineral-trapping of CO_2 than Bandera Brown Sandstone (e.g., the average CO_2 trapped in mineral was ~4 kg for each m^3 medium of Bandera Grey Sandstone, while it was ~2 kg for each m^3 medium of Bandera Brown Sandstone at the end of the 400-year storage period (Figure 5).

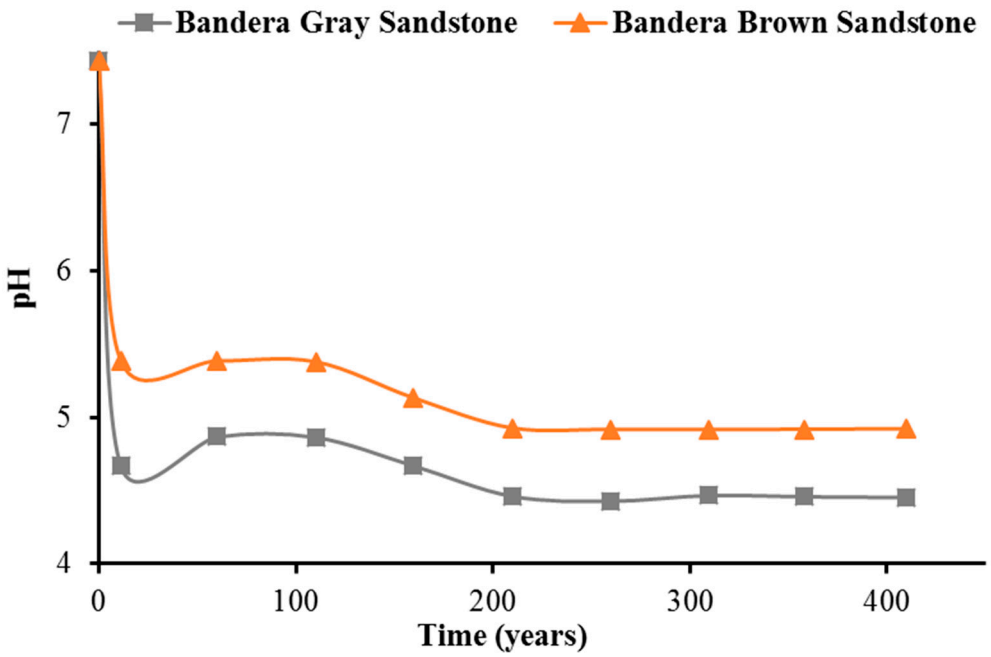

Figure 4. Brine pH for the high and low clay-content sandstone with storage time.

3.4. Effect of Clay Content on Porosity Evolution

It is well verified the sandstone porous media's potential increase in porosity due to CO_2 injection. Even though clay content can substantially vary in different sandstones, its influence on porosity evolution during CO_2 sequestration has not been well investigated. Thus, here, we studied the effect of clay content on porosity variation during CO_2 sequestration using two different sandstones. Our results demonstrate that there is a slight increase in the sandstone porosity and permeability during the storage period (Figure 6). This porosity increase is also a function of the clay content (i.e., the high content sandstone has a high increase in porosity). For instance, the porosity of the Bandera Grey Sandstone scenario is increased by 5.6%, while the porosity of the Bandera Brown Sandstone scenario is increased by only 4.4%, at the end of the storage period (400 years). In summary, we conclude that sandstone clay content has a significant effect on associated geochemical reactions (dissolution and precipitation), pH reduction, porosity evolution and the mineral-trapping capacity. Importantly, clay swelling and mineral breakdown and precipitation are both responsible for changes in porosity. Figure 3 shows that porosity reduces when precipitation predominates and increases when mineral dissolution predominates.

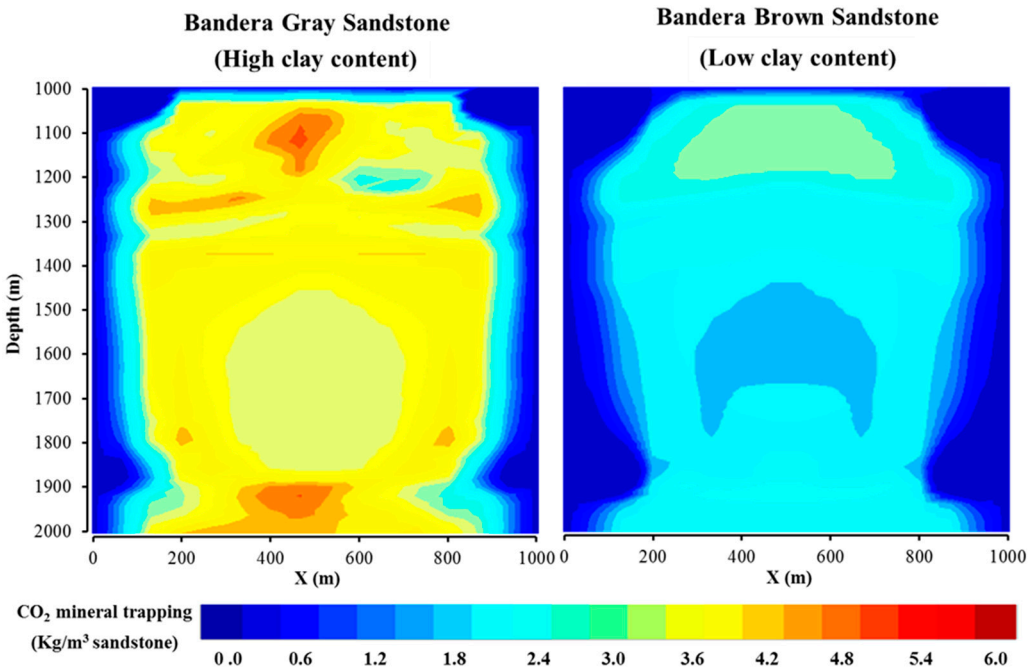

Figure 5. Sequestered in Minerals ($SMCO_2$) for the high and low clay-content sandstones after 400 years post-injection time.

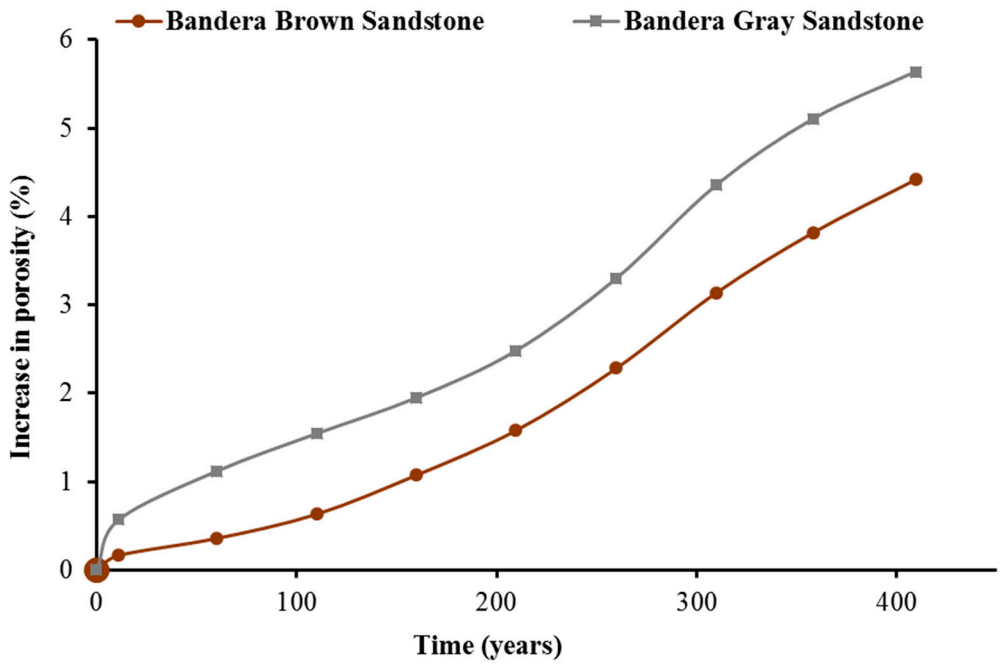

Figure 6. Porosity variations for the high and low clay-content sandstones with storage time.

3.5. Effect of Clay Content on CO_2 Plume Extension

CO_2 plume extension is influenced by a number of variables, including rock wettability, reservoir heterogeneity, formation temperature, brine salinity, injection well type, and the CO_2-water injection scheme [37,38,42–50]. Here, we studied the effect of sandstone clay content on CO_2 plume behaviour (Figure 7).

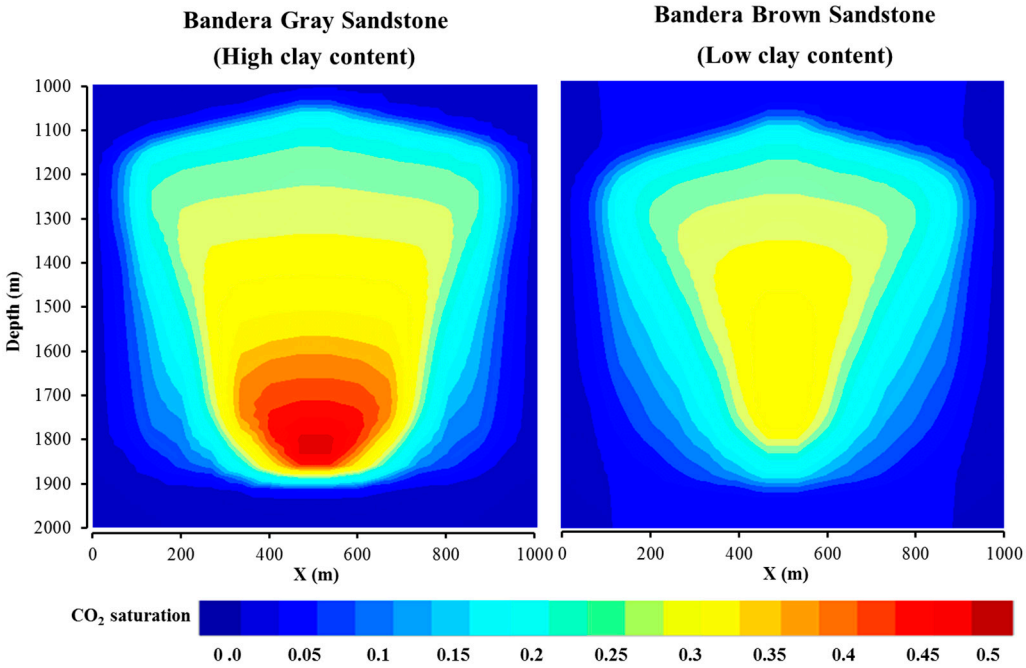

Figure 7. Free CO_2 plume behavior for the high and low clay-content sandstones at the end of injection time, showing that CO_2 remains in the gas phase and rises over time to the top of the model.

Our results showed that the clay content affects the free CO_2 saturation, plume shape and migration behaviour in the sandstone reservoir and that a higher clay-content sandstone has a higher free CO_2 saturation, and a larger CO_2 plume extension (Figure 7).

4. Conclusions

The injection of CO_2 into deep reservoirs is a technology that has the potential to enhance oil recovery from oil reservoirs and cut greenhouse gas emissions [1]. A chemical reaction between the formation rock and the resulting carbonated brine occurs frequently when CO_2 is injected into deep geological formations [51–53]. This chemical reaction leads to mineral dissolution–precipitation, which could affect the rock petrophysical properties [22,23]. Sandstone rocks were typically thought to be less reactive with CO_2 because they contain more quartz than carbonate rocks [24,25]. Nevertheless, sandstones usually contain a significant quantity of cementing and clay components in addition to quartz [26,27]. These substances will interact and disintegrate when they come into contact with CO_2. For instance, Xie et al. [28] discovered that adding CO_2 marginally increased the sandstone's porosity while just slightly increasing its permeability. Moreover, due to mineral involvement or fine migration, CO_2 injection reduces the rock's permeability by 15 to 30% [38]. Also, laboratory tests on sandstone samples showed that the sample permeability is decreased because the quartz and clay that are loosening during the dissolution of the cementing material in the sandstone cause the closure of pore spaces near the sample discharge [38]. Moreover, it was discovered that this sandstone is prone to mineral dissolution and migration at different permeabilities [31]. The composition of the reservoir rock minerals influences the variation in porosity and permeability caused by CO_2 injection. Reactive minerals were anticipated to be less prevalent in sandstone deposits than their carbonate equivalents. However, the evolution of rock characteristics may differ because different sandstone rocks contain varying proportions of clay. Although the clay content can vary substantially in various sandstones, the impact of the clay content on the reservoir scale CO_2-water-rock interactions, brine pH, porosity evolution and mineral-trapping capacity have not been well understood yet. Thus, in this paper, we investigated the effect of clay content on CO_2-water-sandstone interactions, the amount of CO_2 sequestered in minerals, porosity, and brine pH during the CO_2 injection and storage

in sandstone reservoirs. To do so, we simulated two different sandstones: Bandera Grey Sandstone (high clay content) and Bandera Brown Sandstone (low clay content).

Our results showed that the clay contents of sandstone influence the mineral reactions of the sandstone formations during CO_2 storage. However, the low-clay sandstone has a higher precipitations of quartz and a lower dissolution of chlorite. Moreover, based on our findings, the pH of the formation brine is decreased as a result of CO_2 injection into sandstone reservoirs by ~3 units for the high clay-content sandstone and by ~2.5 for the low clay-content sandstone. We also found that the increasing the clay content of the sandstone leads to increasing Mineral-trapping capacity. Furthermore, we found that throughout the storage time, CO_2 injection in the sandstone reservoir increases the sandstone's porosity; this porosity increase is a function of clay content (i.e., higher clay-content sandstone has a higher increase in the porosity). Thus, we concluded that the clay contents of sandstones influence the mineral reactions (dissolution and precipitation) of the sandstone reservoirs, the reduction of the formation brine pH, the mineral-trapping capacity of CO_2, and the increase of sandstone porosity. Thus, we conclude that high clay-content sandstone has a higher mineral-trapping efficiency.

Author Contributions: Conceptualization, E.A.A.-K. and D.S.M.; methodology, E.A.A.-K. and S.I.; software, E.A.A.-K.; validation, E.A.A.-K. and Y.Y.; formal analysis, D.S.M.; investigation, E.A.A.-K.; resources, E.A.A.-K. and Y.Y.; data curation, D.S.M.; writing—original draft preparation, E.A.A.-K.; writing—review and editing S.I.; visualization, D.S.M. All authors have read and agreed to the published version of the manuscript.

Funding: This research received no external funding.

Data Availability Statement: Data is contained within the article.

Conflicts of Interest: The authors declare no conflict of interest.

References

1. Lebedev, M.; Zhang, Y.; Sarmadivaleh, M.; Barifcani, A.; Al-Khdheeawi, E.; Iglauer, S. Carbon geosequestration in limestone: Pore-scale dissolution and geomechanical weakening. *Int. J. Greenh. Gas Control* **2017**, *66*, 106–119. [CrossRef]
2. Yu, H.; Zhang, Y.; Lebedev, M.; Han, T.; Verrall, M.; Wang, Z.; Al-Khdheeawi, E.; Al-Yaseri, A.; Iglauer, S. Nanoscale geomechanical properties of Western Australian coal. *J. Pet. Sci. Eng.* **2017**, *162*, 736–746. [CrossRef]
3. Metz, B.; Davidson, O.; De Coninck, H.C.; Loos, M.; Meyer, L. *IPCC, 2005: IPCC Special Report on Carbon Dioxide Capture and Storage. Prepared by Working Group III of the Intergovernmental Panel on Climate Change*; Cambridge University Press: Cambridge, UK; New York, NY, USA, 2005; 442p.
4. Underschultz, J.; Boreham, C.; Dance, T.; Stalker, L.; Freifeld, B.; Kirste, D.; Ennis-King, J. CO_2 storage in a depleted gas field: An overview of the CO2CRC Otway Project and initial results. *Int. J. Greenh. Gas Control* **2011**, *5*, 922–932. [CrossRef]
5. Zhao, Y.; Wu, S.; Chen, Y.; Yu, C.; Yu, Z.; Hua, G.; Guan, M.; Lin, M.; Yu, X. CO_2-Water-Rock Interaction and Pore Structure Evolution of the Tight Sandstones of the Quantou Formation, Songliao Basin. *Energies* **2022**, *15*, 9268. [CrossRef]
6. Shi, J.; Durucan, S. CO_2 storage in deep unminable coal seams. *Oil Gas Sci. Technol.* **2005**, *60*, 547–558. [CrossRef]
7. Pan, Z.; Connell, L.D. Impact of coal seam as interlayer on CO_2 storage in saline aquifers: A reservoir simulation study. *Int. J. Greenh. Gas Control* **2011**, *5*, 99–114. [CrossRef]
8. Li, Q.; Fei, W.; Liu, X.; Wei, X.; Jing, M.; Li, X. Challenging combination of CO_2 geological storage and coal mining in the Ordos basin, China. *Greenh. Gases Sci. Technol.* **2014**, *4*, 452–467. [CrossRef]
9. Fauziah, C.A.; Al-Yaseri, A.; Al-Khdheeawi, E.; Jha, N.K.; Abid, H.R.; Iglauer, S.; Lagat, C.; Barifcani, A. Effect of CO_2 flooding on the wettability evolution of sand-stone. *Energies* **2021**, *14*, 5542. [CrossRef]
10. Lackner, K.S. A guide to CO_2 sequestration. *Science* **2003**, *300*, 1677–1678. [CrossRef] [PubMed]
11. Iglauer, S.; Paluszny, A.; Pentland, C.H.; Blunt, M.J. Residual CO_2 imaged with X-ray micro-tomography. *Geophys. Res. Lett.* **2011**, *38*, L21403. [CrossRef]
12. Krevor, S.C.M.; Pini, R.; Li, B.; Benson, S.M. Capillary heterogeneity trapping of CO_2 in a sandstone rock at reservoir conditions. *Geophys. Res. Lett.* **2011**, *38*, L15401. [CrossRef]
13. Iglauer, S.; Pentland, C.; Busch, A. CO_2 wettability of seal and reservoir rocks and the implications for carbon geo-sequestration. *Water Resour. Res.* **2015**, *51*, 729–774. [CrossRef]
14. Anchliya, A.; Ehlig-Economides, C.A. Aquifer management to accelerate CO_2 dissolution and trapping. In Proceedings of the SPE International Conference on CO_2 Capture, Storage, and Utilization, San Diego, CA, USA, 2–4 November 2009; Society of Petroleum Engineers: Richardson, TX, USA, 2009.

15. Spycher, N.; Pruess, K.; Ennis-King, J. CO_2-H_2O mixtures in the geological sequestration of CO_2. I. Assessment and calculation of mutual solubilities from 12 to 100 °C and up to 600 bar. *Geochim. Cosmochim. Acta* **2003**, *67*, 3015–3031. [CrossRef]
16. Iglauer, S. *Dissolution Trapping of Carbon Dioxide in Reservoir Formation Brine—A Carbon Storage Mechanism*; INTECH Open Access Publisher: London, UK, 2011.
17. Bachu, S.; Gunter, W.; Perkins, E. Aquifer disposal of CO_2: Hydrodynamic and mineral trapping. *Energy Convers. Manag.* **1994**, *35*, 269–279. [CrossRef]
18. Xu, T.; Apps, J.A.; Pruess, K. Mineral sequestration of carbon dioxide in a sandstone–shale system. *Chem. Geol.* **2005**, *217*, 295–318. [CrossRef]
19. Kweon, H. Mineralogical and Petrophysical Changes in Carbon Dioxide Sequestration. Ph.D. Thesis, The University of Utah, Salt Lake City, UT, USA, 2015.
20. Black, J.R.; Carroll, S.A.; Haese, R.R. Rates of mineral dissolution under CO_2 storage conditions. *Chem. Geol.* **2015**, *399*, 134–144. [CrossRef]
21. Carroll, S.A.; McNab, W.W.; Dai, Z.; Torres, S.C. Reactivity of Mount Simon sandstone and the Eau Claire shale under CO_2 storage conditions. *Environ. Sci. Technol.* **2012**, *47*, 252–261. [CrossRef]
22. DePaolo, D.J.; Cole, D.R. Geochemistry of geologic carbon sequestration: An overview. *Rev. Mineral. Geochem.* **2013**, *77*, 1–14. [CrossRef]
23. Iglauer, S.; Sarmadivaleh, M.; Al-Yaseri, A.; Lebedev, M. Permeability evolution in sandstone due to injection of CO_2-saturated brine or supercritical CO_2 at reservoir conditions. *Energy Procedia* **2014**, *63*, 3051–3059. [CrossRef]
24. Qi, R.; LaForce, T.C.; Blunt, M.J. Design of carbon dioxide storage in aquifers. *Int. J. Greenh. Gas Control* **2009**, *3*, 195–205. [CrossRef]
25. Krevor, S.C.M.; Pini, R.; Zuo, L.; Benson, S.M. Relative permeability and trapping of CO_2 and water in sandstone rocks at reservoir conditions. *Water Resour. Res.* **2012**, *48*, W02532. [CrossRef]
26. Nightingale, M.; Johnson, G.; Shevalier, M.; Hutcheon, I.; Perkins, E.; Mayer, B. Impact of injected CO_2 on reservoir mine ralogy during CO_2-EOR. *Energy Procedia* **2009**, *1*, 3399–3406. [CrossRef]
27. Liu, L.; Suto, Y.; Bignall, G.; Yamasaki, N.; Hashida, T. CO_2 injection to granite and sandstone in experimental rock/hot water systems. *Energy Convers. Manag.* **2003**, *44*, 1399–1410. [CrossRef]
28. Xie, Q.; Saeedi, A.; Piane, C.D.; Esteban, L.; Brady, P.V. Fines migration during CO_2 injection: Experimental results interpreted using surface forces. *Int. J. Greenh. Gas Control* **2017**, *65*, 32–39. [CrossRef]
29. Sayegh, S.G.; Krause, F.F.; Girard, M.; DeBree, C. Rock/fluid interactions of carbonated brines in a sandstone reservoir: Pembina Cardium, Alberta, Canada. *SPE Form. Eval.* **1990**, *5*, 399–405. [CrossRef]
30. Othman, F.; Yu, M.; Kamali, F.; Hussain, F. Fines migration during supercritical CO_2 injection in sandstone. *J. Nat. Gas Sci. Eng.* **2018**, *56*, 344–357. [CrossRef]
31. Tang, Y.; Lv, C.; Wang, R.; Cui, M. Mineral dissolution and mobilization during CO_2 injection into the water-flooded layer of the Pucheng Oilfield, China. *J. Nat. Gas Sci. Eng.* **2016**, *33*, 1364–1373. [CrossRef]
32. Xu, T.; Sonnenthal, E.; Spycher, N.; Pruess, K. TOUGHREACT—A simulation program for non-isothermal multiphase reactive geochemical transport in variably saturated geologic media: Applications to geothermal injectivity and CO_2 geological sequestration. *Comput. Geosci.* **2006**, *32*, 145–165. [CrossRef]
33. Pruess, K. *ECO2N: A TOUGH2 Fluid Property Module for Mixtures of Water, NaCl, and CO_2*; Lawrence Berkeley National Laboratory: Berkeley, CA, USA, 2005.
34. Pruess, K.; Spycher, N. ECO2N–A fluid property module for the TOUGH2 code for studies of CO_2 storage in saline aquifers. *Energy Convers. Manag.* **2007**, *48*, 1761–1767. [CrossRef]
35. Nghiem, L.; Shrivastava, V.; Kohse, B.F.; Hassam, M.; Yang, C. Simulation and optimization of trapping processes for CO_2 storage in saline aquifers. *J. Can. Pet. Technol.* **2010**, *49*, 15–22. [CrossRef]
36. Doughty, C. Modeling geologic storage of carbon dioxide: Comparison of non-hysteretic and hysteretic characteristic curves. *Energy Convers. Manag.* **2007**, *48*, 1768–1781. [CrossRef]
37. Al-Khdheeawi, E.A.; Vialle, S.; Barifcani, A.; Sarmadivaleh, M.; Iglauer, S. Impact of reservoir wettability and heterogeneity on CO 2-plume migration and trapping capacity. *Int. J. Greenh. Gas Control* **2017**, *58*, 142–158. [CrossRef]
38. Al-Khdheeawi, E.A.; Vialle, S.; Barifcani, A.; Sarmadivaleh, M.; Iglauer, S. Influence of CO_2-wettability on CO_2 migration and trapping capacity in deep saline aquifers. *Greenh. Gases Sci. Technol.* **2017**, *7*, 328–338. [CrossRef]
39. Al-Khdheeawi, E.A.; Vialle, S.; Barifcani, A.; Sarmadivaleh, M.; Iglauer, S. Influence of Rock Wettability on CO_2 Migration and Storage Capacity in Deep Saline Aquifers. *Energy Procedia* **2017**, *114*, 4357–4365. [CrossRef]
40. Van Genuchten, M.T. A closed-form equation for predicting the hydraulic conductivity of unsaturated soils. *Soil Sci. Soc. Am. J.* **1980**, *44*, 892–898. [CrossRef]
41. Mualem, Y. A new model for predicting the hydraulic conductivity of unsaturated porous media. *Water Resour. Res.* **1976**, *12*, 513–522. [CrossRef]
42. Al-Khdheeawi, E.A.; Vialle, S.; Barifcani, A.; Sarmadivaleh, M.; Iglauer, S. Influence of injection well configuration and rock wettability on CO_2 plume behaviour and CO_2 trapping capacity in heterogeneous reservoirs. *J. Nat. Gas Sci. Eng.* **2017**, *43*, 190–206. [CrossRef]

43. Al-Khdheeawi, E.A.; Vialle, S.; Barifcani, A.; Sarmadivaleh, M.; Iglauer, S. Effect of brine salinity on CO_2 plume migration and trapping capacity in deep saline aquifers. *APPEA J.* **2017**, *57*, 100–109. [CrossRef]
44. Al-Khdheeawi, E.A.; Vialle, S.; Barifcani, A.; Sarmadivaleh, M.; Iglauer, S. Effect of wettability heterogeneity and reservoir temperature on CO_2 storage efficiency in deep saline aquifers. *Int. J. Greenh. Gas Control.* **2018**, *68*, 216–229. [CrossRef]
45. Al-Khdheeawi, E.A.; Vialle, S.; Barifcani, A.; Sarmadivaleh, M.; Iglauer, S. Impact of injected water salinity on CO_2 storage efficiency in homogenous reservoirs. *APPEA J.* **2018**, *58*, 44–50. [CrossRef]
46. Al-Khdheeawi, E.A.; Vialle, S.; Barifcani, A.; Sarmadivaleh, M.; Iglauer, S. Impact of Injection Scenario on CO_2 Leakage and CO_2 Trapping Capacity in Homogeneous Reservoirs. In Proceedings of the Offshore Technology Conference Asia, 2018, Kuala Lumpur, Malaysia, 20–23 March 2018; 2018.
47. Al-Khdheeawi, E.A.; Vialle, S.; Barifcani, A.; Sarmadivaleh, M.; Iglauer, S. Enhancement of CO_2 trapping efficiency in heterogeneous reservoirs by water-alternating gas injection. *Greenh. Gases Sci. Technol.* **2018**, *8*, 920–931. [CrossRef]
48. Al-Khdheeawi, E.A.; Vialle, S.; Barifcani, A.; Sarmadivaleh, M.; Iglauer, S. The effect of $WACO_2$ ratio on CO_2 geo-sequestration efficiency in homogeneous reservoirs. *Energy Procedia* **2018**, *154*, 100–105. [CrossRef]
49. Al-Khdheeawi, E.A.; Vialle, S.; Barifcani, A.; Sarmadivaleh, M.; Iglauer, S. Effect of the number of water alternating CO_2 injection cycles on CO_2 trapping capacity. *APPEA J.* **2019**, *59*, 357–363. [CrossRef]
50. Al-Khdheeawi, E.A.; Vialle, S.; Barifcani, A.; Sarmadivaleh, M.; Zhang, Y.; Iglauer, S. Impact of salinity on CO_2 containment security in highly heterogeneous reservoirs. *Greenh. Gases: Sci. Technol.* **2018**, *8*, 93–105. [CrossRef]
51. Mahdi, D.S.; Al-Bayati, D.; Saeedi, A.S.; Myers, M.; White, C. Mechanisms of Miscible and Immiscible $scCO_2$ Displacement Efficiency: Analytical Evaluation of Experimental conditions. *Iraqi J. Oil Gas Res.* **2022**, *2*, 98–107. [CrossRef]
52. Al-Bayati, D.; Al-Khdheeawi, E.; Saeedi, A.; Myers, M.; Xie, Q. Investigations of Miscible Water Alternating Gas Injection Efficiency in Layered Sandstone Porous Media. *Iraqi J. Oil Gas Res.* **2022**, *2*, 31–44. [CrossRef]
53. Al-Khdheeawi, E.A.; Mahdi, D.S.; Ali, M.; Fauziah, C.A.; Barifcani, A. Impact of caprock type on geochemical reactivity and mineral trapping efficiency of CO_2. In Proceedings of the Offshore Technology Conference Asia, Kuala Lumpur, Malaysia, 2–6 November 2020; OnePetro: Richardson, TX, USA, 2020.